JOURNAL OF CATALYSIS 142, 641–654 (1993)

A Mössbauer Spectroscopy Study of Platinum–Tin Reforming Catalysts

M. C. HOBSON, JR., S. L. GORESH, AND G. P. KHARE[1]

Engelhard Corporation, Research and Development, Iselin, New Jersey 08830

Received November 9, 1992; revised March 19, 1993

Mössbauer spectroscopy measurements were made to observe alloy formation and interaction of tin with the alumina support in two Pt–Sn/alumina catalysts. The catalysts were rich in tin with an atomic ratio of Pt : Sn = 0.7 : 1. One was prepared by coimpregnation and the other by a sequential impregnation technique. Spectra of samples reduced in a stream of 10% H_2 in argon gave evidence of a solid solution of tin in platinum with a composition approaching Pt_3Sn for most reduction conditions. A large fraction of the tin, 70–80%, interacted strongly with the alumina and did not alloy with the platinum. Two stannous species were identified in the nonalloyed fraction. One was produced by strong interaction with the alumina and the other was a surface ion. Steaming produced large stable crystallites including the intermetallic, Pt_3Sn, and SnO_2. The spectroscopic data were supported by TPR measurements. The results show that platinum and some of the tin reduce between 400 and 700°K with formation of the alloy. The remaining tin reduces to the stannous state between 800 and 850°K.

INTRODUCTION

The bimetallic catalysts, alumina-supported platinum–rhenium and platinum–tin, have captured a major share of the petroleum reforming market by virtue of their enhanced stability and improved selectivity for higher octane gasoline (*1–4*). The role of the base metal is controversial. Tin may affect the catalytic properties and redispersion of the platinum by alloy formation, and modify the acidic characteristics of the support. Selectivity appears to correlate with alloy composition. Sintering may be inhibited by phase separation of SnO_2 and PtO_2 during reoxidation of a Pt–Sn alloy. Such a redispersion mechanism would account for improved stability of the bimetallic.

Characterization of Pt–Sn reforming catalysts in both the oxidized and reduced states have made extensive use of Mössbauer spectroscopy (*5–14*), EXAFS (*15, 16*), XRD (*16–18*), XPS (*16, 19–22*), TPR (*20, 23–26*), and TEM (*27–29*). Interpretations of the results have led to conflicting conclusions concerning formation of platinum–tin alloys and reaction of tin with the support. These Mössbauer parameters are given in Table 1. The data from Gray and Farha (*5*) and Pakhomov *et al.* (*13*) are included although both used a zinc aluminate spinel as a support instead of γ-alumina. The support made a significant difference in the tin spectra. A strong peak at 1.9 mm/sec assignable to PtSn was found for the $ZnAl_2O_4$-supported catalysts which was not a prominent feature in the alumina catalysts.

The results of these studies (*5–14*) differ in detail but have some features in common. The stannic species cannot be completely reduced to lower valence states, at least not after one or two redox cycles. In fresh, calcined samples the stannic species has been identified as small crystallites of SnO_2 (*5–12*). Redox cycling tends to broaden the SnO_2 peak and shift it to more positive velocities. Gray and Farha have interpreted this observation as the reaction of Sn^{4+} with alumina to form $SnAl_2O_5$ (*5*). The magnitude of the isomer shift, IS = 0.12

[1] Present address: Phillips Petroleum Company, Bartlesville, OK 74004.

0021-9517/93 $5.00

TABLE 1

Mössbauer Parameters of Tin Compounds Reported in Reduced $Pt–Sn/Al_2O_3$ Catalysts

Compound	Mössbauer Parameter			Ref.
	IS (mm/sec)	QS (mm/sec)	W (mm/sec)	
Sn(II)(surf)	3.5–3.8	1.35–1.25	1.15 for S_2; 0.94 for S_1	(7)
$SnAl_2O_4$	3.1–3.5	2.2–2.15	0.9; 0.9	
Sn(II) in lattice	4.1	0	1.0	
Pt_3Sn	1.45–1.55	0	1.1–1.15	
PtSn	1.78–1.98	0	1.3–1.4	
$PtSn_4$	2.3–2.5	0	1.0–1.15	
Sn(IV)(surf)	0.4–0.8	0	1.3–1.4	
SnO_2(surf)	0.0–0.05	0.6–0.65	1.4–1.5	
H_2SnCl_6	0.58	0	1.4	(8)
$PtSn_4$	2.34	0	1.8	
PtSn	1.95	4.22	0.7–0.75	
Pt : Sn 85 : 15	1.41	0.73	1.0–1.4	
PtSn	1.92	0.30	1.4	
PtSn	1.97	4.26	0.9–1.2	
PtSn	0.69	1.88	1.2	
SnO or $Sn(OH)_2$	2.82	2.57	0.9–1.2	
$PtSn_4$	2.30	0	1.4	
$SnCl_4 \cdot nH_2O$	0.32	0	1.5	
Sn(IV) as prep.	0.26	0.6	—	(5)
Sn(IV) reduced	0.4–0.7	0	—	
SnO	3.2	2.1	—	
PtSn	2.0	0	—	
Sn(IV)	No parameters quoted			(13)
Sn(II)	3.1	2.1	—	
PtSn	1.93	0	—	
$(SnCl_3)^-$ads	3.60	1.41	—	(6)
	3.70	1.30	—	
Pt_xSn_y	1.64	0	—	
	2.03	0	—	
SnO_2	0.30	0	—	
	0.54	0	—	
$SnCl_2$	4.52	0	—	
SnO–Pt	2.26	1.30	—	
SnO	2.60	1.05	—	

mm/sec, is much less than the half-width of the SnO_2 peak and may be nothing more than experimental error, particularly for microcrystalline stannic oxide. The stoichiometric compound, $SnAl_2O_5$, may not exist. It has not been identified by X-ray diffraction. On the other hand, SnO_2 has been identified by X-ray and electron diffraction on some Pt–Sn catalysts with relatively large crystallites (*26, 27, 29*).

Absorption peaks of the stannous species tend to dominate the overall spectrum in reduced samples. Gray and Farha assigned a doublet in the spectrum of a catalyst reduced with hydrogen at 773°K to stannous aluminate, $SnAl_2O_4$, Table 1, but they could not obtain an X-ray diffraction pattern to support the assignment. A similar doublet has also been assigned to this compound by Kuznetsov *et al.* (*7*) and Legasov *et al.* (*30*). The only XRD data on $SnAl_2O_4$ have been reported by Spandau and Ullrich (*31*). They synthesized stannous aluminate by reacting SnO with α-alumina at 1773°K and found $SnAl_2O_4$ to be a cubic spinel with a unit cell constant of 8.12 Å. A second stannous doublet has been observed in reduced samples and assigned by Berndt *et al.* (*6*) to an adsorbed $SnCl_3^-$ species and by Kuznetsov *et al.* (*7*) to a surface Sn^{2+} species. The assignments have not been confirmed, but, clearly, two stannous species exist on the surface of the reduced catalyst.

Finding evidence of alloy formation in these platinum–tin catalysts is a challenging endeavor. The Mössbauer spectrum of metallic tin is a single peak centered at 2.6 mm/sec relative to stannic oxide. As tin alloys with platinum, the peak shifts towards lower velocities as the atomic percentage of platinum increases (*32–35*). A plot of peak position is a linear function of atomic percent tin (*32*). Unfortunately, the spectral region for the peak positions of platinum–tin alloys is superimposed on the spectral region covered by the low velocity peaks of stannous doublets (*36, 37*). Since stannous ions dominate the spectra of reduced catalysts, identification of alloys by deconvolution of peaks in the 1.3 to 2.0 mm/sec region is difficult. However, the presence of Pt_3Sn, PtSn, and $PtSn_4$ identified by deconvolution of Mössbauer spectra of reduced catalysts has been claimed by Bacaud *et al.* (*8*) and Kuznetsov *et al.* (*7*). These alloys have been identified also by X-ray and electron diffraction techniques (*17, 18, 27–29*).

The conclusions in most of the literature are that tin exists on the support as Sn^{4+} and Sn^{2+} in an oxide environment and as Sn^0 in the form of an alloy with the platinum. The relative amounts of each species will depend on the support material, the method of preparation, and the thermal his-

tory of the sample. The impact each of these variables has on alloy formation is controversial. Apparently, the form of the alumina does not affect alloy formation. Berndt *et al.* (*6*) used η-alumina, while Kuznetsov *et al.* (*7*) and Bacaud *et al.* (*8*) used γ-aluminas. The Berndt and Kuznetsov spectra are virtually identical. Pretreatments by all three were similar, calcination and reduction by hydrogen at 773°K. Methods of preparation differed. Berndt *et al.* used co-impregnation and sequential impregnation in the preparation of two samples, but the Mössbauer spectra were very similar for both. Kuznetsov *et al.* used co-impregnation with a solution containing a Pt–Sn chloride complex. Bacaud *et al.* used sequential impregnation. Alloy formation is more evident in the results of Bacaud than in the Berndt or Kuznetsov spectra. This is unexpected since sequential impregnation should produce less intimate contact of platinum with tin and, consequently, a smaller probability of alloy formation.

In this study we examine conditions of reduction and steaming under which platinum-rich catalysts form solid solutions and intermetallics, and attempt to resolve some of the conflicting results.

EXPERIMENTAL

Catalyst Preparation

Two catalyst samples were prepared with a nominal composition of 0.36 wt% platinum and 0.34 wt% tin on a γ-alumina (Condea) with a surface area of about 200 m^2/g. The tin was approximately 50% enriched in ^{119}Sn. Catalyst A was prepared by sequential impregnation similar to the procedure described by Bacaud *et al.* (*8*). The alumina was impregnated with a hydrochloric acid solution of stannous chloride, dried at 383°K, and calcined at 773°K, followed by impregnation with chloroplatinic acid. Catalyst sample B was prepared by coprecipitation from a HCl solution containing both platinum and tin chlorides following a procedure similar to that described by Gray and Farha (*5*).

Mössbauer Measurements

The Mössbauer spectrometer was a Ranger Scientific Model MS-900 equipped with a 20-mCi Sn-119m radiation source from Amersham, Inc. The MS-900 is a constant acceleration spectrometer operating in either the flyback or triangular mode. It is interfaced to a 1024-channel analyzer and controlled by an IBM PC-XT. The detector is a thin NaI scintillation detector with a 5-mil palladium filter for the ^{119}Sn X-rays. The spectrometer was calibrated with a calcium stannate/beta-tin reference. All isomer shifts are reported relative to calcium stannate. Lorentzian profiles were fitted to the experimental data using a constrained fitting program from Ranger Scientifc. The standard deviation of peak positions in the spectra was ± 0.06 mm/sec or less.

A Mössbauer variable temperature cryostat was built to our specifications by Cryo industries. The temperature can be set between 77 and 300°K by a thermal switch between the LN2 and a cold finger for coarse adjustment and an electrical heater on the cold finger for fine adjustment. The heater is powered by a 15-vdc power supply and controlled with an Omega Series 6000 controller and platinum resistance thermometer attached to the cold finger.

The two catalyst samples were pressed into 13-mm wafers, approximately 1 mm thick. These wafers were placed in a boron nitride sample holder attached to the cold finger of the Mössbauer cryostat and spectra taken at room temperature and liquid nitrogen temperature. The wafers were removed from the sample holder, placed in a gas-tight transfer tube, and reduced by a flowing mixture of 7% hydrogen/argon. After reduction the samples were transferred to the boron nitride sample holder in a glove box free of oxygen, sealed in the holder, and then moved to the Mössbauer cryostat. Spectra were recorded at several temperatures between 77 and 300°K. The samples underwent several redox cycles as the temperature of reduction was increased

from 473 to as high as 950°K. At some of the higher temperatures water vapor was added to the reducing gas stream to produce a H_2/H_2O ratio of 2.

Temperature-Programmed Reduction

The TPR experiments were made on an in-house built unit, controlled by an IBM PS/2 computer. Hydrogen uptake was measured by a thermal conductivity detector. Approximately 160 mg of each sample was dried *in situ* at 373°K for 1 hr in an argon gas stream at 50 ml/min. After drying, the temperature was lowered to 198°K by manually adding liquid nitrogen. The gas stream was then switched to 10% hydrogen in argon at 50 ml/min. The sample was held at 198°K for 15 min to allow for baseline adjustment and then the temperature was ramped to 1123°K at 10°K/min. The samples was held at the final temperature for 10 min. The data were reduced using PeakFit software by Jandel Scientific.

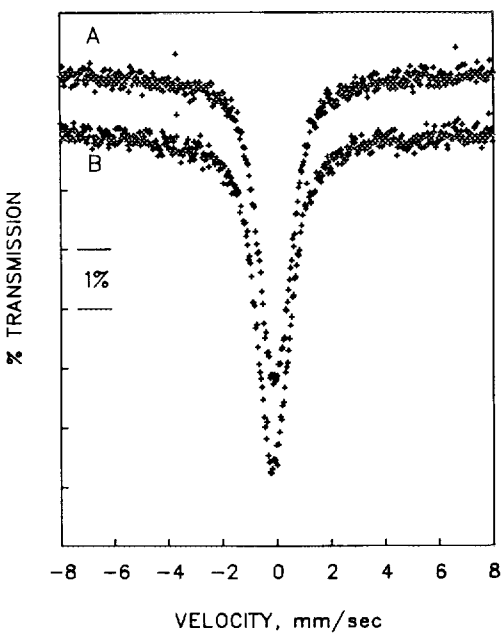

FIG. 1. Mössbauer spectra of catalysts A and B calcined at 773°K.

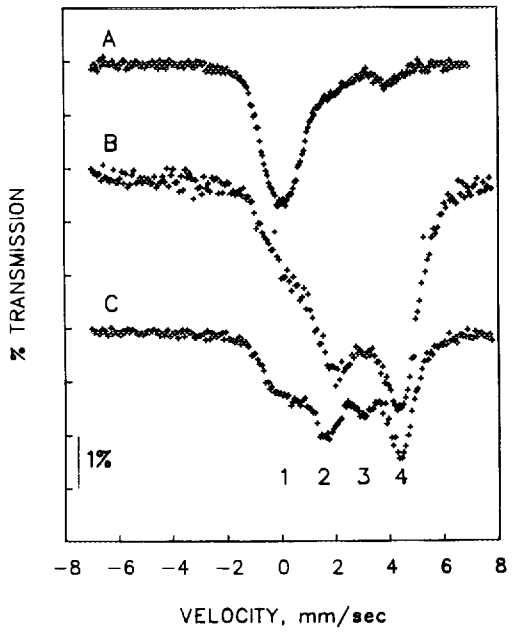

FIG. 2. Mössbauer spectra of catalyst A reduced with 7% H_2 in argon. (A) reduced at 473°K, (B) reduced at 773°K, and (C) reduced at 823°K.

RESULTS

The room-temperature spectra of the fresh catalysts are shown in Fig. 1. Each show a single, broad peak centered near zero velocity that is typical of a stannic ion in an oxide environment with cubic symmetry. As expected, the tin exists only as SnO_2 or a stannic oxide-like species.

Sample A was reduced at 473°K for 2 hr. At this reduction temperature a SnO species begins to appear, Fig. 2A, with an isomer shift, IS = 2.94 ± 0.03 mm/sec and a quadrupole splitting, QS = 2.09 ± 0.03 mm/sec. The bulk of the tin remains as SnO_2 with IS = 0.06 ± 0.01 mm/sec and a large half-width, HWHM = 0.87 mm/sec. The sample reduced at 473°K was exposed to air at room temperature for 1 hr, reduced at 798°K for 1 hr, exposed to air again at room temperature for 1 hr, and reduced at 823°K for 1 hr. Spectra were recorded after each reduction in the redox cycles, Figs. 2B and 2C, respectively. Spectra of catalyst B

reduced from 1 to 3 hr at temperatures between 773 and 823°K were very nearly identical to catalyst A spectra.

The observable peaks are labeled 1 through 4 in Fig. 2. About 20% of the original Sn^{4+} species, peak 1, remains with no significant change in its Mössbauer parameters. From left to right, peaks 2, 3, and 4 cover the region where spectra of stannous species are found. The peak positions measured at room temperature for peaks 2, 3, and 4 were identical for both catalysts reduced at 823°K, 1.73 ± 0.04, 3.06 ± 0.06, and 4.35 ± 0.03 mm/sec, respectively. Peak 2 has a large half-width, suggesting that two peaks are superimposed on each other.

Peak 3 appears to increase in relative intensity with increasing time and temperature of reduction and is very sensitive to oxygen during reoxidation of the reduced catalyst. These results suggest that peak 3, probably one-half of a doublet, should be assigned to a surface Sn^{2+} species.

Spectra of the samples were recorded at temperatures between 77 and 300°K. The

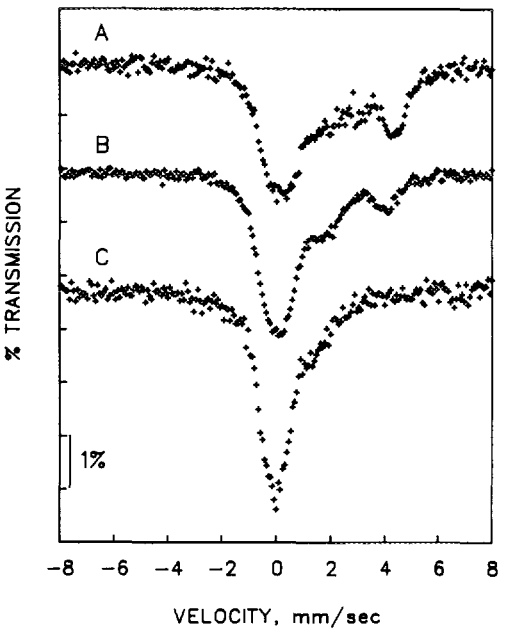

FIG. 4. Mössbauer spectra of catalyst B reduced with 7% H_2/3% H_2O in argon. (A) reduced at 793°K, (B) reoxidized in air at room temperature, and (C) reduced at 893°K and reoxidized in air at room temperature.

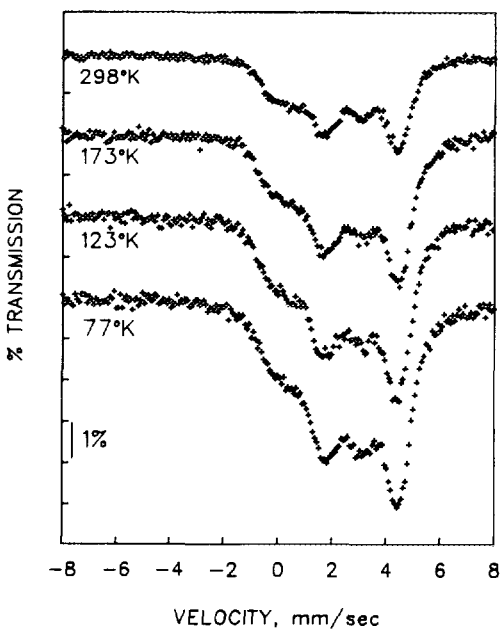

FIG. 3. Mössbauer spectra of catalyst A reduced at 823°K measured as a function of sample temperature.

results for sample A reduced at 823°K are shown in Fig. 3. As expected the areas under the peaks assigned to Sn^{2+} species increased with decreasing sample temperature relative to Sn^{4+} species, but no new peaks were resolved. The spectra as a function of temperature of sample B were similar except for small variations of the relative areas under the peaks. Small positive shifts in the Sn^{2+} peaks of 0.07 mm/sec on going from room temperature to LN_2 temperature are of the order expected for changes in lattice constant and are, in fact, within experimental error for these samples. No phase changes have occurred.

Fresh samples of both catalysts were pretreated under steaming conditions to determine if differences might appear when sintering occurred. Catalyst B was heated at 790°K for 3 hr in a stream of reforming gas saturated with water vapor at room temperature. The sample was only partially reduced, Fig. 4A. Much of the tin remained

as a stannic species as seen by the large peak remaining near 0 mm/sec. Only some small part was reduced to a stannous species. The stannous portion of the spectrum is similar to that obtained without water vapor present in the hydrogen stream. This sample was exposed to air for approximately 2 hr and some but not all of the stannous material was re-oxidized to a stannic species, Fig. 4B. Spectrum B is similar to that of the low-temperature reduction of catalyst A, Fig. 2A, except for the area asymmetry of the doublet. Contrary to results shown in Fig. 2A, the area under the peak near 2 mm/sec is much larger than that near 4 mm/sec. Clearly, some of the tin may be alloying with the platinum. Increasing the pretreatment temperature of catalyst B to approximately 893°K for 3 hr and exposing to air for 2 hr produced spectrum C in Fig. 4. Although the stannous species reoxidized to stannic, the spectrum shows a shoulder at 1.55 mm/sec which is characteristic of Pt_3Sn. An alloy has formed under conditions expected to sinter the platinum. This sample was set aside in air for approximately 5 weeks and run again. The shoulder at 1.55 mm/sec could no longer be observed.

Sample A was subjected to a similar treatment at elevated temperatures. In this case, the highest temperature reached was 950°K. The spectrum of this sample in the reduced state, spectrum A, Fig. 5, is similar to spectrum C, Fig. 2, of this catalyst reduced at lower temperatures without water vapor in the gas stream. Reoxidation of this sample by exposing it to air at room temperature for 1 hr gave spectrum B, Fig. 5. Alloy formation is indicated by the large area of the peak at about 1.7 mm/sec relative to the peak at 4.1 mm/sec. If only a Sn^{2+} species remained, a peak with a relatively small area should have appeared at about 2 mm/sec.

The reduced catalysts contain two stannous species. One exhibits strong interaction with the support and is assigned to a doublet with peaks at about 2 and 4.1 mm/sec. We will refer to it as a Sn–O–Al or SnO-like species. The second is assigned to a surface species, Sn^{2+} (surf) with peaks at about 3.1 and 4.5 mm/sec.

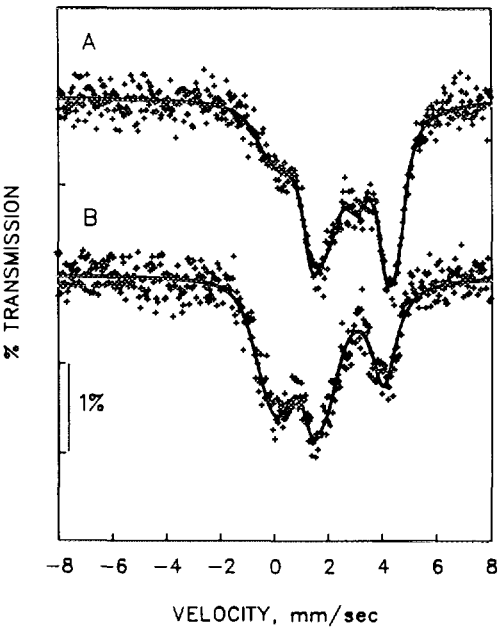

FIG. 5. Mössbauer spectra of catalyst A reduced with 7% H_2/3% H_2O in argon. (A) reduced at 953°K and (B) reoxidized in air at room temperature.

Once peak positions and half-widths of the two stannous doublets were obtained the deconvolution of a spectrum could be completed. For room-temperature spectra, peak positions of the Sn–O–Al doublet were constrained to fall between 2.0 and 2.1 mm/sec and between 4.0 and 4.1 mm/sec. Peak positions of the surface doublet were constrained to fall between 3.0 and 3.2 mm/sec and 4.4 and 4.6 mm/sec. Deconvolution of spectra of most reduced samples could be completed by just two additional peaks. Individual peaks and their sum are shown in Fig. 6 for catalyst B reduced at 823°K. The six Lorentzians were used to fit all the spectra of reduced samples. Four peaks were used for partially reduced or reoxidized samples where the 3.1 mm/sec peak was absent. The peak at zero velocity was the Sn^{4+} species some of which was always

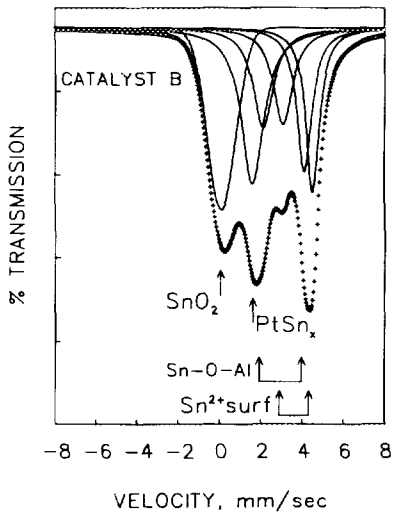

FIG. 6. Deconvolution of the Mössbauer spectrum of catalyst B reduced at 823°K showing the six fitted peaks identifying the species SnO_2, $PtSn_x$, Sn–O–Al, and Sn^{2+}(surf).

present in the reduced catalyst. The most reasonable assignment of the other peak was to Pt_3Sn or a solid solution of tin in platinum. The results of the curve fitting are given in Tables 2 and 3.

The results of the temperature programmed reduction of catalyst A are shown in Fig. 7. The data have been corrected for baseline shifts and detector bias voltage. The seven Gaussian peaks used to fit the data have maxima at 417, 462, 515, 662, 846, 897, and 986°K. The TPR spectrum of catalyst B was similar with peaks at 412, 469, 526, 651, 834, 883, and 975°K. The first four peaks are associated with reduction of PtO_2 and some of the SnO_2 in intimate contact with the platinum. The peak at 846°K is reduction of SnO_2 not in contact with the platinum. The two peaks at high temperatures are reduction of contaminants, such as sulfur. XPS spectra of the two catalysts detected low levels of sulfate ions. Burch (*26*) reported two peaks in the TPR of tin on alumina. The high-temperature peak was at about 850°K which correlates well with the peak at 846°K in Fig. 7. He also observed a peak at 960°K for alumina containing 0.6% sulfur as sulfate, and found this peak shifted to lower reduction temperatures on impregnation with tin. Therefore, we attribute the two high-temperature peaks to sulfate contamination.

DISCUSSION

The spectra of catalysts A and B reduced in flowing hydrogen at temperatures be-

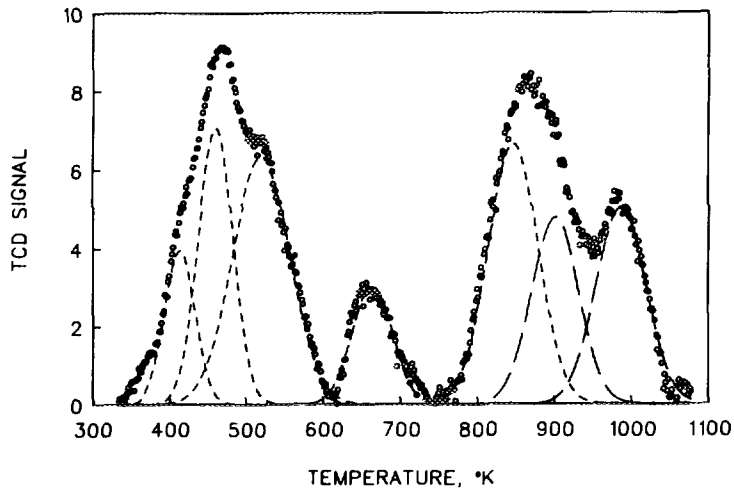

FIG. 7. TPR profile of fresh Pt–Sn/Al_2O_3 catalyst A. The individual Gaussian peaks have maxima at 417, 462, 515, 662, 846, 897, and 986°K.

TABLE 2

Mössbauer Parameters of Catalysts A and B Reduced with 7% Hydrogen in Argon

Catalyst	Figure	Temperature (°K)		IS (mm/sec)	QS (mm/sec)	Assignment
		Reduce	Measure			
A	2A	473	298	0.06		SnO_2
				2.94	2.09	Sn–O–Al
	2B	773	298	0.07		SnO_2
				1.66		Pt_3Sn
				3.22	1.85	Sn–O–Al
				4.00	1.35	Sn^{2+}(surf)
	2C, 3A	823	298	0.03		SnO_2
				1.55		Pt_3Sn
				3.2	2.03	Sn–O–Al
				3.83	1.49	Sn^{2+}(surf)
	3B	823	173	0.04		SnO_2
				1.59		Pt_3Sn
				3.19	2.23	Sn–O–Al
				3.91	1.55	Sn^{2+}(surf)
	3C	823	123	0.01		SnO_2
				1.61		Pt_3Sn
				3.21	2.14	Sn–O–Al
				3.92	1.49	Sn^{2+}(surf)
	3D	823	77	0.02		SnO_2
				1.72		Pt_3Sn
				3.28	2.02	Sn–O–Al
				3.90	1.53	Sn^{2+}(surf)
B	6	823	298	0.10		SnO_2
				1.61		Pt_3Sn
				3.11	2.00	Sn–O–Al
				3.76	1.44	Sn^{2+}(surf)

TABLE 3

Mössbauer Parameters of Catalysts A and B Reduced with 7% Hydrogen/3% Water in Argon

Catalyst	Figure	Temperature (°K)		IS (mm/sec)	QS (mm/sec)	Assignment
		Reduce	Measure			
B	4A	793	298	0.09		SnO_2
				1.58		Pt_3Sn
				3.10	2.08	Sn–O–Al
				3.84	1.46	Sn^{2+}(surf)
	4B		298	0.02		SnO_2
				2.91	2.16	Sn–O–Al
	4C	893	298	−0.04		SnO_2
				1.55		Pt_3Sn
A	5A	953	298	−0.01		SnO_2
				1.38		$PtSn_x$
				3.04	2.21	Sn–O–Al
				3.79	1.48	Sn^{2+}(surf)
	5B		298	0.03		SnO_2
				1.44		$PtSn_x$
				3.04	2.07	Sn–O–Al

tween 773–823°K, Fig. 2, are virtually identical to spectra of reduced catalysts reported by Berndt *et al.* (*6*) and Kuznetsov *et al.* (*7*), but differ somewhat with Bacaud *et al.* (*8*), Fig. 8. The results of Berndt *et al.* are not shown in the figure since they are identical to those of Kuznetsov. The evidence for alloy formation in the Bacaud spectrum, a shoulder at 1.6 mm/sec, is not so clear in the others. Although the spectra from these several studies are similar, the interpretation of the results and assignment of spectral features to specific tin species differ significantly. In the following discussion we interpret the Mössbauer data by specifying only four tin species and show that this is consistent with results reported using other measurement techniques.

Reduction and Support Interactions

The low temperature reduction of catalyst A, Fig. 2A, produced a stannous doublet with peak area asymmetry. The ratio of the area under the low velocity peak to that of the high velocity peak is 0.73. Partial reoxidation of the same sample after reduction and steaming, Fig. 5B, again produced two peaks in the stannous ion region. However, the area ratio is now 1.57 and the low-velocity peak is unusually wide. Two or more tin species must contribute to the low-velocity peak. This peak was deconvoluted into peaks at 1.44 and 2.00 mm/sec. The area ratio of the 2 mm/sec-to-4 mm/sec peaks is 0.88 and the isomer shift and quadrupole splitting are 3.04 and 2.07 mm/sec, respectively. These two stannous species, 2A and 5B, are identical. Sintering would account for the small difference in the ratios. The ratio approaches one as the sample is cooled to 77°K. This area asymmetry and its temperature dependence are characteristics of vibrational anisotropy, the Goldanski–Karyagin Effect, at the site of the Mössbauer isotope.

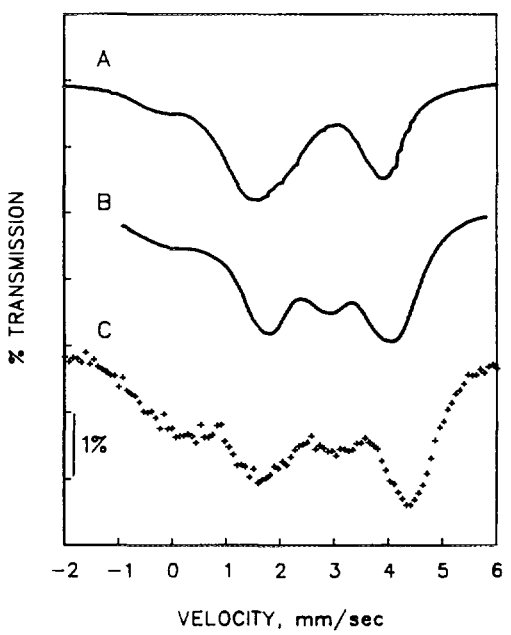

FIG. 8. Comparison of Mössbauer spectra of similar reduced PtSn catalysts. (A) from Bacaud, Fig. 4a, Ref. (*8*); (B) from Kuznetsov, Fig. 2(B-5), Ref. (*7*); C, this study, Fig. 2C. Spectra A and B reproduced with permission from Academic Press.

The stannous doublet produced by low temperature reduction has been observed also by several investigators (*5–8, 30, 38–40*). It was assigned to $SnAl_2O_4$, Table 1 by Gray and Farha (*5*), Kuznetsov *et al.* (*7*) and Legasov *et al.* (*30*). Since attempts at confirming the assignment by X-ray diffraction were not successful (*5*), formation of a stoichiometric compound has not been established.

Suzdalev and co-workers (*38–40*) studied the interaction of stannous ions with the surface of silica gel, mordenite, and molybdenum oxide. Suzdalev *et al.* (*38*) found an area ratio of 0.8 for Sn^{2+} ion exchanged onto silica gel. From this, using the method suggested by Flinn, Ruby, and Kehl (*41*), they calculated the root mean square displacement normal to the SiO_2 surface to be 1.9 times larger than parallel to the surface. Spectrum A, Fig. 2, is identical to the spectrum of supported SnO reported by Suzdalev in his analysis, Fig. 4 in Ref. (*38*). By analogy the vibrational anisotropy of our sample is a little larger, and implies a high dispersion of tin on the alumina support.

On mordenite in which stannous ions had

replaced sodium ions, an isomer shift, IS = 3.4 mm/sec, and a quadrupole splitting, QS = 2.1 mm/sec, was obtained. The spectrum for the stannous species was interpreted as interaction of Sn^{2+} ions with the Al^{3+} sites in the mordenite. Suzdalev *et al.* (*39*) ascribe the larger isomer shift observed in the mordenite to a higher ionicity of Sn^{2+} bond at the aluminum exchange site. A similar spectrum was also obtained by Firsova *et al.* (*40*) for stannous species on the surface of a tin–molybdenum oxide catalyst after chemisorption of propylene.

A second stannous species with a peak at 3.1 mm/sec appears at the higher reduction temperatures, Fig. 2. In both catalysts the peak above 4 mm/sec shifted to higher velocities near 4.4 mm/sec and the area under the peak increased. The peak at 3.1 mm/sec must be the low-velocity peak of a doublet with the other half at about 4.4–4.5 mm/sec. The isomer shift is 3.8 mm/sec and the quadrupole splitting is 1.3 mm/sec. On limited exposure to air the peak at 3.1 mm/sec vanishes and the area under peak 4 decreases and shifts back to about 4.1 mm/sec. This doublet was first assigned to a stannous surface species by Kuznetsov *et al.* (*7*). Although Berndt *et al.* (*6*) observed the same stannous doublet, they assigned it to an adsorbed $(SnCl_3)^-$ species. Such an assignment is difficult to support. Kuznetsov found that the doublet remained essentially unchanged after treating a reduced sample with oxygen containing water vapor at 823°K for 12 hr followed by reduction in hydrogen at the same temperature. At the same time the chloride content of the sample decreased from 1.15 to 0.1%. We also found the doublet unchanged after reduction in an H_2/H_2O stream, Figs. 4A and 5A. A tin chloride species would not survive either treatment. We agree with the interpretation of Kuznetsov. It must be produced by a stannous ion in a surface site with a low coordination number that results from removal of surface oxygen by the high-temperature reduction.

Structural information can be derived from the Mössbauer parameters of the two doublets to support the assignments. The interaction of stannous ions with alumina sites increases the isomer shift to 3.2 from 2.6 mm/sec for bulk SnO, and the truncated O_2-lattice at the surface causes a shift to 3.9 mm/sec for the surface stannous ion. The increase in isomer shift measures an increase in *s*-electron density at the nucleus, as shown by the equation.

$$IS = \delta_\alpha = \frac{2\pi Ze^2}{5}\,[|\Psi_a(0)|^2 - |\Psi_s(0)|^2](R_e^2 - R_g^2), \quad (1)$$

where $[R_e^2 - R_g^2]$ is the change in the radius of the nucleus from ground to excited state on absorption of the Mössbauer gamma ray. It is positive for Sn-119. The chemistry is contained in the term $\{|\Psi_a(0)|^2 - |\Psi_s(0)|^2\}$, the difference between the electron density at the nucleus in the absorber and the source. This nuclear electron density comes almost exclusively from *s*-electrons. Indirectly, *p*- and *d*-electrons change the *s*-electron density through screening effects. It is a screening effect that causes the increase in isomer shift from bulk SnO to Sn–O–Al to surface Sn^{2+} ion. Interaction with the more electronegative aluminum ion decreases the electron density in the hybrid *sp*-bonding orbitals of the stannous ion. As a result the screening effect of the 5*p*-orbitals on the *s*-electron density decreases and, consequently, the *s*-electron density at the nucleus increases. A similar argument can be made for the surface stannous ion. Most of the *p*-electron density resides in the p_z-orbital that has expanded normal to the surface. Screening of the 5*s*-electrons by the 5*p*-electrons decreases and the 5*s*-electron density at the nucleus increases. It is surprising that the effect is larger at the surface than in the Sn–O–Al bond.

The quadrupole splitting of the doublets is represented by the formula

$$QS = \frac{1}{2}\,e^2qQ\left(1 + \frac{\eta^2}{3}\right)^{1/2}, \quad (2)$$

where Q is the quadrupole moment of the nucleus, $eq = V_{zz}$ is the principal component in the z direction of the electric field gradient (EFG) tensor, and $\eta = (V_{xx} - V_{yy})/V_{zz}$ is an asymmetry parameter to account for a lack of axial symmetry in the principal components of the EFG. The asymmetry parameter takes on values from 0 (axial symmetry) to 1 ($V_{zz} > V_{xx} > V_{yy}$). There are two contributions to the term q, one from the charges on the atoms in the lattice surrounding the Mössbauer atom, the other from valence electrons in orbitals without cubic symmetry:

$$q = (1 - \gamma_\infty)q_{\text{lat}} + (1 - R)q_{\text{val}}. \quad (3)$$

The coefficients are the appropriate Sternheimer antishielding factors. The q_{lat} and q_{val} terms usually have opposite signs (*42*). The Sn^{4+} ion has a closed shell electron structure and, therefore, q_{lat} will dominate the EFG. On the other hand, Sn^{2+} ions have two electrons in hybridized 5*s*- and 5*p*-orbitals of the valence shell. Although the 5*s*-orbitals are spherically symmetrical and make no valence contribution to q, any unequal distribution of electronic charge in the p orbitals will. The observed quadrupole splittings are QS = 2.2 mm/sec for polycrystalline SnO, QS = 2.4 mm/sec for Sn–O–Al, and QS = 1.1 mm/sec for Sn^{2+} surface. The small increase in QS going from SnO bulk to Sn–O–Al probably represents a large increase in q_{lat} and a small increase in q_{val}. The site symmetry may have changed from tetrahedral in SnO to trigonally distorted octahedral in Sn–O–Al.

The decrease in QS for the Sn^{2+} surface species relative to Sn–O–Al can be explained by the lattice and valence contributions to q at the surface. Assume that Sn^{2+} ions are in tetrahedral surface sites with one oxygen ion missing. The p_z-orbital will expand into space normal to the surface, the energy of the orbital decreases and p-electron density increases preferentially in this orbital. The contribution of the valence shell electrons to q_{val} increases. Since the sign of q_{val} is opposite that of q_{lat} the sum of the two decreases and, consequently, the quadrupole splitting is smaller.

Alloy Formation

The strongest evidence of alloy formation was found when catalyst B was reduced at 893°K in the presence of water vapor followed by re-oxidation. The platinum sinters to crystallites large enough for stable alloy formation, as shown in Fig. 4C. The shoulder at 1.55 mm/sec is assigned to Pt_3Sn based on the Mössbauer measurements on a series of Pt–Sn alloys by Charlton *et al.* (*32*). The alloy slowly reoxidizes in air at room temperature indicating that the platinum has sintered into crystallites large enough to have significant amounts of tin incorporated into a "bulk" phase. This implies that a minimum crystallite size is required for existence of a stable alloy. Further evidence for this has been found in X-ray line broadening data obtained in this laboratory on Pt–Sn reforming catalysts. Shifts in platinum diffraction peaks caused by solid solution of tin in platinum are seldom observed in crystallites of less than 4–5 nm diameter (*43*).

The deconvoluted singlet in most of the reduced samples fell between 1.55 and 1.65 mm/sec. The peak is probably a distribution of compositions represented by $PtSn_x$ where $0 < x < 0.3$ and includes Pt_3Sn. Compositions with $x > 0.3$ were not found. The assignment is based on three observations; the minimum falls in the platinum-rich region of Pt–Sn Mössbauer spectra (*32*), the clearly resolved Pt_3Sn peak in sintered platinum crystallites cited above and the lack of any evidence the peak is part of another stannous ion doublet.

This peak can be used to estimate the amount of alloy formed. Assume that the cross section for capture of Mössbauer gamma radiation by tin alloyed with platinum is a function of the Debye temperature of metallic platinum and not tin. The recoil-free fraction of the $PtSn_x$ should be about 70% of that for the stannic oxide species. Then the area under the peak representing

the platinum–tin alloy relative to the stannic oxide consists of 20% of the total tin present in the sample with one exception. When catalyst A was reduced in the presence of steam at 953°K, the fraction of tin as alloy increased to about 40% of the total. The quantitative estimates of alloy formation, which are supported by TPR results discussed below, are subject to large experimental error. However, the trend in alloy formation on steaming is quite clear from the relative areas of the stannous and alloy peaks.

Catalyst Model

The Mössbauer results suggest the following model. In the oxidized state highly dispersed Pt^{4+} is attached to the alumina surface through a SnO_2-like layer. On reduction between 400 and 500°K the platinum forms microcrystallites of Pt^0 and hydrogen spillover reduces the neighboring Sn^{4+} to Sn^{2+}. At higher temperatures additional Sn^{4+} surrounding the site is reduced to the surface Sn^{2+} species and Sn^{2+} adjacent to the platinum microcrystallites reduces further to form the Pt_3Sn intermetallic. We note that the alloy peak in all the spectra is near 1.56 mm/sec with one exception. The isomer shift for the alloy peak of catalyst A, Table 3, is 1.4 mm/sec. The high temperature reduction in a H_2/H_2O stream must have sintered the platinum to large crystallites and, in effect, diluted the alloy formation by increasing the time and temperature requirements for an even distribution of tin in the crystallite. Residual Sn^{4+} must be isolated clusters of stannic oxide too far removed from platinum sites for hydrogen spillover to be effective. This argument is consistent with the sequential method used in preparation of catalyst A.

The possible phases present during a redox cycle are a Sn(IV) phase, a Sn(II) phase, platinum, and a platinum-rich alloy phase with a composition between 0 and 30 at% Sn. These are the only species required to rationalize the Mössbauer spectra contrary to the six to eight species proposed in the literature (*6–8*).

The TPR results correlate well with the Mössbauer data. Reduction of platinum and some of the tin produces the first three peaks in Fig. 7. Mössbauer spectrum A, Fig. 2, confirms the low-temperature reduction of a fraction of the Sn^{4+} to Sn^{2+}. The TPR peak at 662°K represents reduction of Sn^{2+} to Sn^0, and is driven by formation of a PtSn alloy. The TPR peak at 846°K is assigned to reduction of the remaining Sn^{4+} to Sn^{2+}. It is either stabilized by the alumina or located too far from platinum to form an alloy. The maximum in the relative area of the stannous ion peaks in the Mössbauer spectra occurred in samples reduced at 823°K which correlates well with this TPR peak. Furthermore, an estimate of the fraction of tin forming an alloy compared well to the Mössbauer results. Approximately 25% of the tin alloys as calculated from the areas under the peaks at 662 and 846°K compared to 20% estimated from the Mössbauer data.

Other TPR studies (*20, 23–26*) of Pt–Sn reforming catalysts have reported similar results. The peaks in the TPR spectra are not as well resolved as ours, and, with the exception of the results reported by Burch (*26*), the temperature range did not exceed 873°K. In most cases a broad reduction peak skewed on the high temperature side with a maximum between 450 and 500°K was observed. de Miguel *et al.* (*23*) and Burch (*26*) found a shoulder or an unresolved peak between 625 and 675°K. de Miguel noted that the shoulder was resolved better on a sequentially impregnated sample compared to a co-impregnated one and suggested this indicated better contact between platinum and tin in the co-impregnated sample. In our spectra this peak is completely resolved for both catalysts A and B. In support of our results both Dautzenberg *et al.* (*24*) and Lieske and Volter (*25*) conclude that reduction of tin is catalyzed by intimate contact with platinum, only a small amount of tin alloys with the

platinum and most of the tin reduces only to Sn^{2+}. Dautzenberg *et al.* (*24*) also report that severe oxidation of $Pt–Sn/Al_2O_3$ catalysts produces a separate stannic oxide phase.

The model is consistent with the conclusions in the literature from studies using other techniques (*15, 20, 23–29*). High dispersions of platinum and tin were found by Meitzner *et al.* (*15*) in an EXAFS study of similar catalysts. In the reduced state they found very little evidence for tin-tin or tin-platinum bonding but extensive coordination of tin with oxygen. The Pt–Pt coordination number was 3.2 compared to 7.2 for a Pt/Al_2O_3 catalyst. They conclude that the tin promotes the dispersion of the platinum by formation of small clusters of platinum atoms bonded through Sn^{2+} ions to the alumina. They did not find evidence of a solid solution of tin in platinum. Their method of $Pt–Sn/Al_2O_3$ preparation; formation of a gel from an $AlCl_3$ and $SnCl_4$ solution, calcining and impregnating with chloroplatinic acid, may have produced Pt–Sn clusters with insufficient tin to easily form an alloy. In fact, they point out that the metal clusters in the catalyst involve only a small fraction of the total tin.

Studies of $Pt–Sn/Al_2O_3$ catalysts by TEM and microdiffraction techniques (*27–29*) have shown the formation of several intermetallics in reduced samples. Handy *et al.* (*27*) found a core/shell morphology in the oxidized state with SnO_2 covering a platinum core. Reduction produced PtSn. These results were reversible on reoxidation. Similar TEM and microdiffraction findings were reported by Chojnacki and Schmidt (*29*), and PtSn was found in XRD measurements by Srinivasan *et al.* (*28*). Most of these observations were on relatively large crystallites, 5–20 nm, and Pt/Sn ratios of 1 : 1 to 1 : 3.

CONCLUSIONS

A model for platinum-tin reforming catalysts based on the analysis of Mössbauer spectra has been developed that is consistent with the literature including TPR, XRD, TEM, and EXAFS studies. The highly dispersed bimetallic in the oxidized state consists of small clusters of PtO_2 anchored to the alumina surface through a SnO_2-like intermediate layer. On undergoing reduction the platinum forms microcrystallites of Pt^0 and hydrogen spillover from the platinum reduces the Sn^{4+} to Sn^{2+}. At reduction temperatures above 700°K some of the Sn^{2+} reduces further and forms a solid solution and/or intermetallics with the platinum. The composition of the alloy is a function of the relative amounts of platinum and tin in the catalyst and the thermal history of the sample. Most of the tin does not alloy. About 70–80% of it remains as Sn^{2+} ions that interact strongly with the alumina support. Reoxidation converts all of the Sn^{2+} to Sn^{4+}, and oxidation of the tin in the alloy promotes the redispersion of the platinum to clusters of PtO_2 anchored to the alumina surface through SnO_2-like species. If redox conditions are severe enough to sinter the platinum, reoxidation produces crystallites of platinum with a surface of PtO_2 surrounded by crystallites SnO_2. A large fraction of the tin will only reduce at high temperatures above 800°K. An optimum Pt/Sn ratio for selectivity implies an optimum alloy composition. Removal of tin from the alloy-forming phase by strong interaction with the support shifts the composition toward platinum-rich alloys and decreases the selectivity. Deactivation results from these sintering and support interaction processes.

ACKNOWLEDGMENTS

We wish to acknowledge Professor Gary L. Haller and Drs. D. R. Anderson and S. M. Levine for many helpful discussions, Dr. D. R. Anderson and W. Schultz for design and construction of the TPR hardware and software, Inga Kirejevas for help in preparation of the manuscript, and Engelhard Corporation for permission to publish this work.

REFERENCES

1. Sinfelt, J. H., "Bimetallic Catalysts: Discoveries, Concepts, and Applications." Wiley, New York, 1983.

2. German Offenlegungsschrift 2,027,296 (1970) to Shell.
3. Burch, R., and Garla, L. C., *J. Catal.* **71,** 360 (1981).
4. Karpinski, Z., and Clarke, J. K. A., *J. Chem. Soc. Faraday Trans.* **71,** 893 (1975).
5. Gray, P. R., and Farha, F. E., *in* "Mössbauer Effect Methodology," Vol. 10. Plenum, New York, 1976.
6. Berndt, H., Mehner, H., Volter, J., and Meisel, W., *Z. Anorg. Allg. Chem.* **429,** 47 (1977).
7. Kuznetsov, V. I., Belyi, A. S., Yurchenko, E. N., Smolikov, M. D., Protasova, M. T., Zatolokina, E. V., and Duplyakin, V. K., *J. Catal.* **99,** 159 (1986).
8. Bacaud, R., Bussiere, P., and Figueras, F., *J. Catal.* **69,** 339 (1981).
9. Bacaud, R., Bussiere, P., Figueras, F., and Mathieu, J. P., *in* "Preparation of Catalysts" (B. Delmon, P. A. Jacobs, and G. Poncelet, Eds.). Elsevier, Amsterdam, 1976.
10. Kuznetsov, V. I., Yurchenko, E. N., Belyi, A. S., Zatolokina, E. V., Smolikov, M. A., and Duplyakin, V. K., *React. Kinet, Catal. Lett.* **21**(3), 419 (1982).
11. Li, Yong-Xi, and Hsia, Yuan-Fu, *Hyperfine Interact.* **28,** 875 (1986).
12. Klabunde, K. J., Li, Yong-Xi, and Purcell, K. F., *Hyperfine Interact.* **41,** 649 (1988).
13. Pakhomov, N. A., Buyanov, R. A., Moroz, E. M., Yurchenko, E. N., Chernyshev, A. P., Zaitseva, N. A., and Kotelnikov, G. R., *React. Kinet, Catal. Lett.* **14,** 3229 (1980).
14. Li, Y-X., Klabunde, K. J., and Davis, B. H., *J. Catal.* **128,** 1 (1991).
15. G. Meitzner, Via, G. H., Lytle, F. W., Fung, S. C., and Sinfelt, J. H., *J. Phys. Chem.* **92,** 2925 (1988).
16. Li, Y-X., and Klabunde, K. J., *J. Catal.* **126,** 173 (1990).
17. Srinivasan, R., DeAngeles, R. J., and Davis, B. H., *J. Catal.* **106,** 449 (1987).
18. Srinivasan, R., DeAngeles, R. J., and Davis, B. H., *Catal. Lett.* **4,** 303 (1990).
19. Adkins, S. R., and Davis, B. H., *J. Catal.* **89,** 371 (1984).
20. Sexton, B. A., Hughes, A. E., and Foger, K., *J. Catal.* **88,** 466 (1984).
21. Balakrishnan, K., and Schwank, J., *J. Catal.* **127,** 287 (1991).
22. Baronetti, G. T., de Miguel, S. R., Scelza, O. A., and Castro, A. A., *Appl. Catal.* **24,** 109 (1986).
23. de Miguel, S. R., Baronetti, G. T., Castro, A. A., and Scelza, O. A. *Appl. Catal.* **45,** 61 (1988).
24. Dautzenberg, F. M., Helle, J. M., Biloen, P., and Sachtler, W. M. H., *J. Catal.* **63,** 119 (1980).
25. Lieske, H., and Volter, J., *J. Catal.* **90,** 96 (1984).
26. Burch, R., *J. Catal.* **71,** 348 (1981).
27. Handy, B. E., Dumesic, J. A., Sherwood, R. D., and Baker, R. T. K., *J. Catal.* **124,** 160 (1990).
28. Srinivasan, R., Rice, L. A., and Davis, B. H., *J. Catal.* **129,** 257 (1991).
29. Chojnacki, T. P., and Schmidt, L. D., *J. Catal.* **129,** 473 (1991).
30. Legasov, V., Fabritchnyi, P., Demazeau, G., Afanasov, M., Shvyriaev, A., and Hagenmuller, P., *C.R. Acad. Sci. Paris* **306,** 879 (1988).
31. Spandau, H., and Ullrich, T., *Z. Anorg. Chem.* **274,** 271 (1953).
32. Charlton, J. S., Cordey-Hayes, M., and Harris, I. R., *J. Less-Common Met.* **20,** 105 (1970).
33. Kanekar, C. R., Rao, K. P., and Rao, V. U. S., *Phys. Lett.* **19,** 1995 (1965).
34. Bryukhanov, V. A., Delyagin, N. N., Kuz'min, R. N., and Shpinel, V. S., *Zh. Eksper. Teor. Fiz.* **46,** 1996 (1966).
35. Ibraimov, N. S., and Kuz'min, R. N., *Sov. Phys. Dok.* **10,** 1071 (1966).
36. Cordey-Hayes, M., *J. Inorg. Nucl. Chem.* **26,** 915 (1964).
37. Davies, C. G., and Donaldson, J. D., *J. Chem. Soc. A*, 946 (1968).
38. Suzdalev, I. P., Goldanskii, V. I., Makarov, E. F., Plachinda, A. S., and Korytko, L. A., *Sov. Phys. JETP* **22,** 979 (1966).
39. Suzdalev, I. P., Plachinda, A. S., and Makarov, E. F., *Sov. Phys. JEPT* **26,** 897 (1968).
40. Firsova, A. A., Khovanskaya, N. N., Tsyganov, A. D., Suzdalev, I. P., and Margolis, L. Ya., *Kinet. Katal.* **12,** 708 (1971).
41. Flinn, P. A., Ruby, S. L., and Kehl, W. L., *Science* **143,** 1434 (1964).
42. Ingalls, R., *Phys. Rev. A* **133,** 787 (1964).
43. St. Amand, J. R., personal communication.